Proceedings of the 2006 IEEE International Conference on Robotics and Automation
Orlando, Florida - May 2006

A Hands-On-Robot for Accurate Placement of Pedicle Screws

T. Ortmaier, H. Weiss, U. Hagn, M. Grebenstein, M. Nickl, A. Albu-Schäffer,
C. Ott, S. Jörg, R. Konietschke, Luc Le-Tien, and G. Hirzinger
German Aerospace Center (DLR e.V.), Institute of Robotics and Mechatronics
D - 82234 Wessling, Germany, e-mail: Tobias.Ortmaier@dlr.de

***Abstract*— This paper presents a novel system for accurate placement of pedicle screws. The system consists of a new light-weight (<10 kg), kinematically redundant, and fully torque controlled robot. Additionally, the pose of the robot tool-center point is tracked by an optical navigation system, serving as an external reference source. Therefore, it is possible to measure and to compensate deviations between the intraoperative and the preoperatively planned pose. The robotic arm itself is impedance controlled. This allows for a new intuitive man-machine-interface as the joint units are equipped with torque sensors: the robot can be moved just by pulling/pushing its structure. The surgeon has full control of the robot at every step of the intervention. The hand-eye-coordination problems known from manual pedicle screw placement can be omitted.**

***Index Terms*— robotic surgery, hands on robotics, soft robotics, navigation, pedicle screw, impedance control**

I. Introduction and Motivation

Robotics is a little more than 30 years old. Nevertheless, many people had expected faster progress in robotic intelligence due to the intense research work worldwide. A lot of pilot schemes with sensor technology and sensor feedback (the basis of all flexible, adaptive behaviour) were stopped for reasons of cost and reliability. Therefore, present-day industrial robots are mostly fast and robust positioning machines which guarantee precision by means of mechanical stiffness and are thus worse than the human arm in their payload to weight ratio (e.g. 1:20). Although the human arm can hardly guarantee positioning or repeat accuracy on its own, it can carry out complex tasks flexibly and reliably by means of the feedback of sensor data (visual and haptic data) even under varying conditions.

The application of mechatronic systems in medicine and especially in operating theatres will become more and more important in the future. This results from the fact that such tasks are assigned to systems which either compensate for the weaknesses of the surgeon or take over assistance functions during an operation. In doing so the different strengths of the surgeon and the mechatronic system can be combined with each other, see Tab. I.

The content of this contribution is a robotic system for the navigated placement of pedicle screws. The main part of this system is a newly developed robot for a wide range of surgical applications. In the approach presented here the robot works semi-autonomously: it controls the alignment of the surgical instrument (here: a drill) by means of intra-operative navigation according to a patient-specific planning. The surgeon takes over the guidance of the robot by means of haptic interaction along appropriate trajectories to the target area (so-called "hands on robotics") and thus keeps full control over the operation process. The goal is therefore the combination of the strengths of surgeon and robot.

TABLE I
Strenghts of man and robot (according to [1]).

Man	Robot
Good hand-eye coordination	High geometric accuracy
High skilfulness	No tremor or fatigue
Flexible and adaptable	Application of defined forces possible
Able to utilise qualitative information	Able to work in hazardous environments
Able to evaluate unclear information	Integration of different sensors and control strategies possible

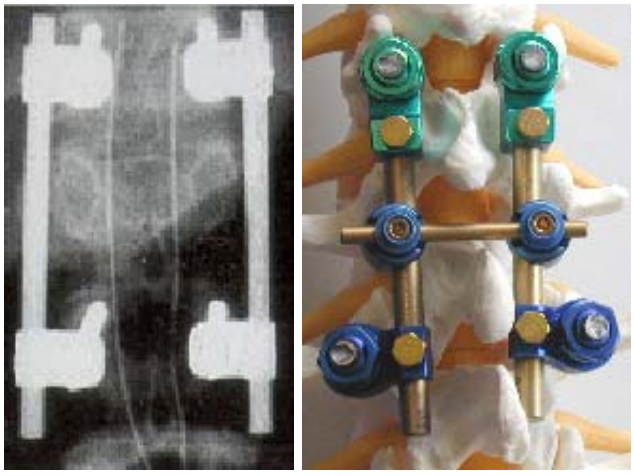

(a) Postoperative X-Ray image (b) Demonstration on model

Fig. 1. Transpedicular fixation with fixateur interne. Figures courtesy of Prof. Beisse (BGU Murnau).

In the following section the potentials arising from the use of a robot are compared with the purely manually performed methods of treatment. In Sect. III the complete system and the workflow of the application are demonstrated. A description of the robot is given in Sect. IV. Finally, an outlook of further developments concludes this article.

II. State of the Art

Serious diseases of the spine such as degeneration-induced slipped discs, instable fractures of the lower thoracic and lumbar spine, or severe spinal defects after tumour resections are increasingly treated with a so-called transpedicular fixation with fixateur interne. In this stabilisation operation screws are placed into the nearest intact vertebral bodies above and below the lesion and stiffened with each other by means of titanium rods (see Fig. 1). The screws are inserted into the vertebral body in pairs, from behind, through the pre-drilled pedicles and transmit the force flow of the spine away from the defect area via the two rigid rods. The screws must be placed very accurately since a penetration, for example, of the spinal canal with damage to the spinal marrow can lead to paraplegia. Ventrally the aorta lies close to the spine. Turning too long screws into the spinal bodies or a slipping with the preparation tools can cause injuries of this artery resulting in perilous haemorrhages.

In case of a conventionally coducted transpedicular fixation the surgeon is only provided with intra-operative 2D X-ray images for the alignment and positioning of the pedicle screws. Postoperative verifications showed that in 10 to 40% faulty screw placement occurred. With the application of navigation systems, which enable an intra-operative, three-dimensional navigation of the instruments, the error rate can be lowered to 2 - 8% [2]–[5].

In the navigation-assisted but manually accomplished therapy the navigation system shows the operator the position of his instruments in relation to pre-operative image data (CT or X-ray) on the screen (see Fig. 2). The optimal pose (position and orientation) of the screws is planned in the CT images. The current pose of the patient's spine is measured by the navigation system by means of reference markers attached to the vertebra. The operator can now accurately (but manually) insert the screws into the pedicles. For this it is necessary to align the planned pose with the measured pose. This requires numerous changes of view direction with frequent new eye accommodations. This leads to very high demands on both the concentration and the spatial sense of the surgeon. An additional source of error is finally the manual execution of the task (such as tremor, complex multi-axis motions, fatigue). Therefore, with a robot-assisted therapy the quality of pedicle screw placement to be expected is higher than with the manual procedure, as the above mentioned sources of error can be avoided.

During the past years a variety of robots for different surgical applications have been introduced, see [6] for an overview. These robots possess different degrees of autonomy. The tele-operated robot is exclusively controlled by the surgeon [7], [8]. Semi-autonomous systems share the task between surgeon and robot. The task execution can be either passive or active. See e. g. the independent alignment of the robot-guided instrument on to a located tumor [9], the Acrobot-system for knee endoprothetics [10], or the robot presented in this article. Finally, some systems offer the complete autonomous execution of assistance functions, as for instance the fully automatic endoscope guidance via real-time image processing [11]. Nevertheless, experiences reported in [10] lead to the conclusion that, the more the surgeon is involved in the surgical workflow the more robot-assisted therapies will experience a greater acceptance.

III. System and Workflow

The combination of robot and navigation system enables an important step for closing the gap in the flow of information between therapy planning and therapy execution. With such a combination the data gained from navigation can be optimally and directly integrated into the therapy with clearly increased accuracy. Figure 2 shows the experimental set-up with the new medical robot for navigated placement of pedicle screws which was built at the DLR. The medical robot is equipped with a linear guide to hold the drive unit of the drill (see Fig. 3). This drive unit can be manually moved along the drill axis. On the one hand a precise guidance of the drill instrument is guaranteed, on the other hand the surgeon receives a haptic feedback of the drill forces that occur during the drilling. Furthermore, the responsibility of the intervention is left to the surgeon, the robot acts as an intelligent instrument holder only.

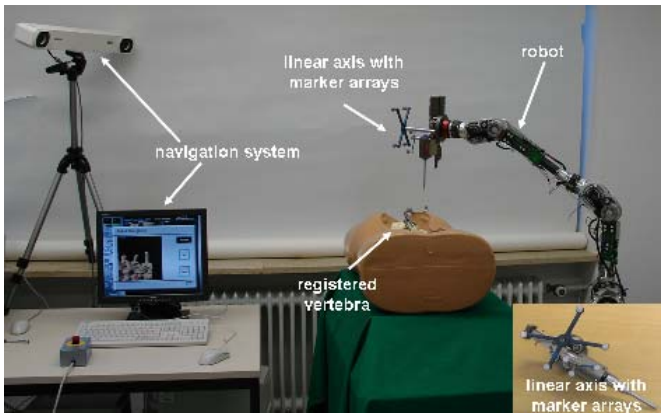

Fig. 2. Experimental set-up for the navigated placement of pedicle screws with the new medical robot and the BrainLAB VectorVision navigation system.

The robot control is coupled with the navigation system via a TCP/IP connection. The stereo camera of the navigation system tracks both the registered vertebra and the four-marker-array attached to the robot. Based on this information the navigation system calculates the relative pose of the vertebra with respect to the drill coordinate frame and sends the data continuously to the robot. The robot control is in different impedance-controlled states according to a mode commanded by the graphic user interface. The robot does

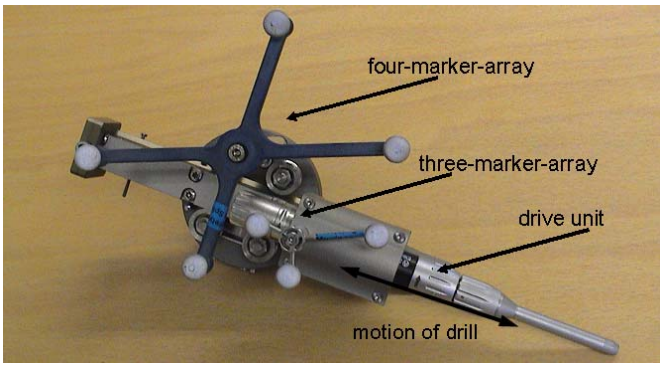

Fig. 3. Linear guide with opical markers.

not actively carry out any movements (with the exception of mode 4) but is guided manually by the user - a fully automatic drilling does not take place. Depending on the active mode, only certain directions of movement along given trajectories are possible. In order to ensure a safe medical application a workflow (i.e. a sequence of modes) was developed which is described in detail in the following.

Before starting with the intervention, both, robot and vertebra need to be registered with respect to their tracking markers. The vertebra is registered by collecting surface points with a tracked pointer which are thereafter matched to the segmented CT data. The drill is registered during **Mode 1**, see below.

Mode 1 (pre-positioning): From its starting position the robot arm is freely manoeuvrable in all directions of the Cartesian space. In this phase the drill tip is registered with an instrument calibration matrix with respect to the four-marker-array, whereby this array (rigidly mounted near the tip of the robot arm) is crucial for the determination of the robot pose. The three-marker-array (mounted on the drive unit) is only used for measuring the drilling depth and is linearly movable with the drive unit relative to the four-marker-array. The user switches to mode 2 if the arm is pre-positioned.

Mode 2 (towards drill axis): The robot only allows movements along trajectory 1 (see Fig. 4) which guides the instrument axis to the pre-planned drill axis (trajectory 2) so that both axes coincide at interception point P. This is carried out by Cartesian impedance control, whereby the direction along trajectory 1 shows zero stiffness and all other degrees of freedom (DoF) possess a high stiffness (see Sect. IV-B on robot control). On reaching the drill axis it is automatically switched to mode 3.

Mode 3 (along drill axis): After the drilling instrument is lying on the drilling axis it is guided by the user along trajectory 2 to the drilling point. The control is analogue to mode 2. Shortly before reaching the drilling point it is automatically switched to mode 4.

Mode 4 (fine tuning): The user now releases the robot

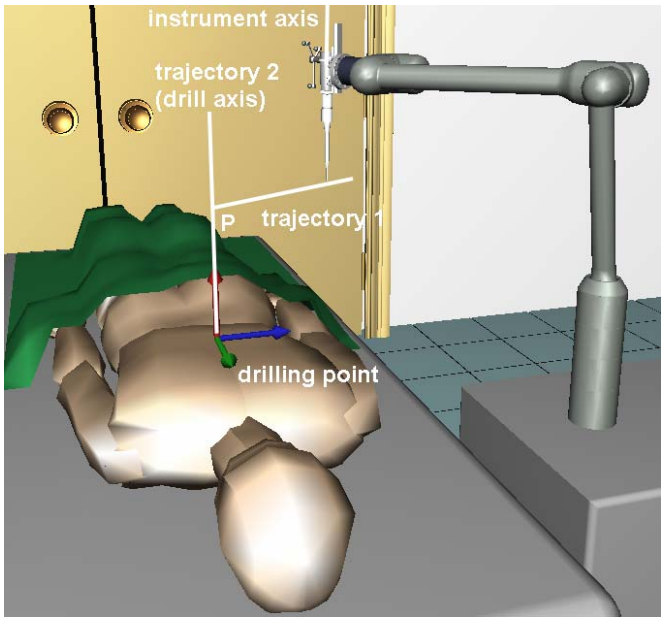

Fig. 4. Implemented workflow: the impedance controlled robot is manually guided by the operator to the drilling point along pre-planned trajectories.

arm. The robot can thus align the pose of the drilling instrument actively, without external disturbances and with highest possible accuracy, based on the current pose measured by the navigation system and the planning data. At this point there is still no contact between robot tip and vertebra. As the robot carries out movements independently and actively in this mode, speed and motion limits are very strict. The flow control allows a switch to mode 5 only if the pose error lies within certain tolerances.

Mode 5 (drilling): The impedance-controlled robot runs with maximum stiffness (this basically corresponds to a position control). The user now manually drills the planned drilling hole with the help of the instrument guidance. The brake on the linear guides is released and the drill moved manually along the instrument axis. The drilling depth is measured by the navigation system on the basis of the relative pose of the four-marker-array with respect to the three-marker-array and displayed graphically to the operator. After the drilling has been carried out the drill is moved back and fixed. The user then switches to mode 6.

Mode 6 (safe removal): The robot arm only allows movements along the drilling axis - for safety reasons only away from the patient. As from 100 mm above the drilling point it is automatically switched to mode 7.

Mode 7 (free motion): The robot arm is now freely manoeuvrable again (as in mode 1). The vertical position, however, is restricted to 100 mm above the drilling point, whereby it is made sure that the drilling instrument can not come into contact with the patient.

IV. Medical Robot

In the following section the design criteria of the robot as well as the considered clinical applications including the workspaces are presented. This analysis forms the basis for the joint design and the number of kinematic DoF. In particular the digital electronics, the communication bus, and the control of the robot are introduced.

A. Arm Design

The design objective of the robot was to build a compact, intuitively operated robot arm for a wide field of medical applications. Besides the classic pre-programmed and tele-manipulated operation, the robot shall also be suited for semi-autonomy where the surgeon can directly interact with the robot.

The joint order of the robot arm and the grouping of the joints (Fig. 5) are based on experiences gained from the DLR light-weight robot development [12]. Investigations of possible fields of application (e.g. visceral surgery, heart surgery, orthopaedics, urology, neurology) of the robot showed a large area where the requirements are similar. A generic robot arm that is tailored to these demands can therefore be used in different areas and thus reduces the costs for robot-assisted surgery.

The required absolute positioning accuracy of the robot in combination with a navigation system was derived from the anatomic conditions for the placement of pedicle screws and is at least 1 mm for translation and 1° for rotation. The accuracy of the robot end-effector was determined by the accuracy demands of bypass surgery and should be better than 0.1 mm for translation and 0.5° for rotation, respectively [13]. Furthermore, the robot end-effector should be able to move with a speed of at least 60 mm/s and $30^\circ/s$ within selected target areas [13]. These values result from the analysis of the requirements for the robot-assisted compensation of remaining movement in beating heart surgery. The considered workspaces enable robot-assisted operations on the ureter, gallbladder and appendix as well as cardiosurgical operations such as heart valve and bypass operations [13] and is the optimal one for minimally invasive surgery procedures (see Fig. 6).

The kinematics of the medical robot was optimised taking into account the above mentioned criteria. The optimisation objective was the minimisation of the sum of the link lengths l_1 and l_2 (see Fig. 5), in order to make the robot design as compact and light as possible. The thus formulated optimisation problem was solved by means of Genetic Algorithms and resulted in $l_1 = 310$ mm and $l_2 = 385$ mm. Besides the requirements due to the application, this optimisation also took into account the motors chosen (see Sect. IV-A.3) and the relative positioning accuracy of the joints including the gear ratios of the harmonic drive gears 1:100, see [13]. (The gear ratio for joints 2/3 were changed after the optimization due to mechanical reasons to 1:60.)

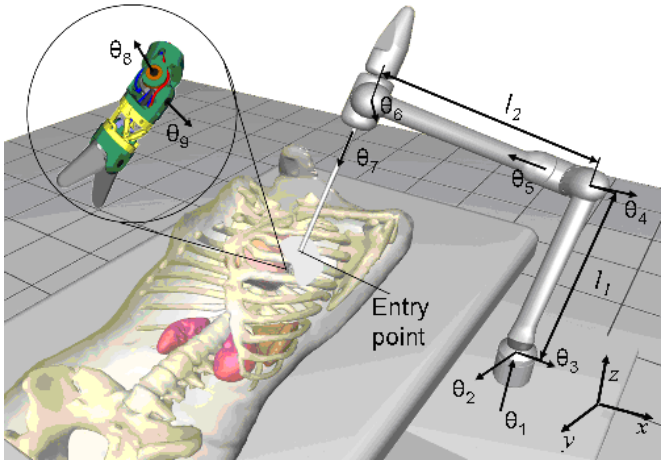

Fig. 5. Kinematic structure of medical robot with l_1 and l_2 to be minimzed (here with instrument for laparoscopic surgery).

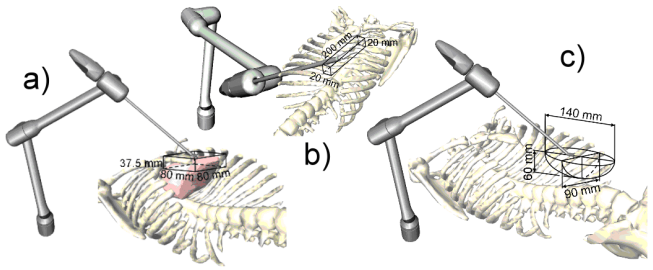

Fig. 6. Typcal applications with workspace: heart surgery (a), harvesting of arteria mammaria interna (b), visceral surgery (c).

To determine the maximum necessary manipulation forces of the robot arm the drilling of holes for pedicle screw placement was taken as a medical reference application. For this purpose experiments took place at the DLR and in the Laboratory for Biomechanics of the Technical University of Munich. At the TU Munich scientists were engaged in the examination of the drill-hole quality dependent on drill and cutter geometries and drilling angles. At the DLR robot-assisted drilling tests were carried out in order to assess the maximum forces with respect to magnitude and distribution. For these purposes the DLR light-weight robot LWR-II was equipped with a linear guide and a drilling instrument. Drilling tests were carried out on a bovine spine (in vitro). The result of these experiments was a maximum force of 30 N ("worst case" examination).

The next two sections describe the implementation of the requirements in the constructive design of the joint units as well as in the design and implementation of the robot control.

1) Robot Hardware: A central goal during the development of the robot was the realisation of a shape that is as slender as possible. This is due to the very restricted space in the operating field and the tight interaction of the surgeon with the robot. As the robotic arm represents an additional system near the operating table, the already extremely limited space thus becomes even more restricted. A slender, compact arm reduces the space conflicts (e.g. risk of collision) and thus increases the acceptance of the robot by the surgeon. The same holds for the direct interaction of the surgeon with the medical robot.

Additional design criteria for the development were derived from the previous experience at the Institute of Robotics and Mechatronics in the field of light-weight robotics (LWR I-III): (a) joint redundancy: a flexible setup in the space-confined operation environment is ensured by 7 joints, (b) torque-controlled joints enable the direct haptic interaction described in Sect. III, (c) a robot weight of less than 10 kg allows a simple handling of the system and reduces the potential risk of injury by collision due to low inertia, and (d) safety of the system by means of sensor redundancy.

Fig. 7. Medical robot with external electronics (without housing).

2) Robot Structure: The focus of the development of the robot structure was on the design of the segments between the joint units. In addition to the load-supporting function the electronics for the joints 4-7 are also to be integrated there. The requirements can be formulated as follows: (a) low outer diameter, (b) light-weight design allowing for a reduction of the joint torques in the lower axes and for easier transport of the system, (c) high rigidity of the components for the minimisation of positioning errors, and (d) good accessibility of the integrated electronics (power electronics, power supply, communication electronics) to improve maintainability. Due to the required good accessibility of the integrated electronics and the longish, slender form, no supporting shell structure (as used e.g. for the DLR light-weight robot III) could be applied. A structure in frame design was preferably used, see Fig. 7.

3) Robot Joints: Similar to the DLR light-weight robot development (LWRI-III), the joints of the medical robot consist of motors and gears, link side torque and position sensors, as well as motor side position sensors and safety brakes. On the one hand this raises the system safety by the use of redundant sensors, on the other hand the sensor values are needed for the control described as follows.

As a requirement for the joint development, a compact and slender joint grouping was derived. Whilst the lower joint unit has three intersecting axes (roll-pitch-pitch), the other two joint units have two intersecting axes each (pitch-roll), see Fig. 5. The intersecting axes in the joints contribute to a simplified robot control as the inverse kinematics of the robot arm has an analytical solution.

Whilst axis 1 of the robot arm is designed analogue to the joints of the LWR-III (cf. [12]), for the realisation of the intersecting axes 2-3, 4-5, and 6-7 a coupled joint design was chosen. One motor drives the output joint 1 via a gear unit. In contrast to this, for the coupled joints two motors, which are connected to each other via gears, actuate the two respective DoF together. In this way a universal joint can be built up, whereby the joint axes intersect each other and both motors are placed on the same segment of the joint unit. Particularly with regard to the joint electronics, this simplifies the joint design considerably as one electronic board drives one joint unit.

The coupling of the drives leads to the fact that movements around each individual joint axes can always only be carried out by interaction of both motors. Therefore, both motor torques are used together if the robot is operated in the preference direction of its joints. On the one hand these directions of preference can be taken into consideration during the preoperative planning of the installation of the robot at the operating table. On the other hand the joint redundancy offers the possibility to position the robot arm in such a way that the directions of preference are used.

In all robot joints a special motor developed by the DLR (DLR-RoboDrive [14]) is used which was optimised for application in robotics with respect to its weight and the electrical losses. In contrast to the established industrial robots, the power electronics of the motors are located directly in the robotic arm and not in the external control unit. This brings advantages for the electromagnetic compatibility (EMC). The EMC-problematic cable currents of the motors are thus generated near the motors and no long transmission cables through the whole robot arm are necessary. The

integrated power electronics in combination with the field-orientated control allow an optimal use of the specialized motors.

B. Robot Control

Differing from the architecture of the DLR light-weight robots, only the current control of the motors is carried out locally in the joint electronics. This controller is implemented on an FPGA (field programmable gate array). Additionally, on the FPGA the communication between the joint units and to the external control computer as well as the joint unit house keeping are implemented (see Fig. 8). The FPGA technology was chosen to achieve a more flexible implementation of the joint controller, a high control rate, and a small sized joint electronics. Furthermore, by means of flexible DSP structures and integrated processing units, modern FPGAs enable the efficient implementation of algorithms (e.g. motor control, end stops) and complex, exception handling mechanisms directly in the joints. Diverse IO standards support the connection of different hardware components (e.g. sensors, motors, brakes). The FPGAs are interlinked with a slim, package-based protocol (HIC, IEEE 1355).

The transparency, modularity, and flexibility of a simple, package-based protocol are particularly suitable for robots used in research. In the past years the IEEE 1355 has been extended and standardised by the ESA as SpaceWire (ECSS-E50-12). By the use of a physical Multi-Gigabit-Transceiver as physical layer, which is included in modern FPGA generations, and by the implementation of the higher layers of the SpaceWire protocol in the FPGA, a very flexible communication infrastructure with a bandwidth of 1 GBit/s and cycle time less than 333 μs was achieved.

The physical communication layer of the joints among each other is implemented with copper conductors (Cu). The connection of the robot to the control computer via optical fibre enables the galvanic decoupling of the equipment and thus the reduction of the patient's leakage currents which is necessary for medical technology. Figure 8 gives an overview of the communication structure. The low latency and the high bandwidth of the communication facilitate the application of standard hardware for controlling the system, as no dedicated signal processors must be integrated into the joint units. All controllers, except for motor current control, are implemented on standard platforms outside the robot. Development costs are thus saved and future hardware updates facilitated.

The calculations are mainly carried out on standard CPUs and not on dedicated hardware. This allows for the application of modern software development tools and methods. The functionality implemented in the FPGA is integrated via an efficient Signal-Flow oriented Middleware, cf. Fig. 9. Based upon this, a functional separation between robot hardware and robot control (Hardware Abstraction Layer) decouples the development processes of hard- and software. Whereas

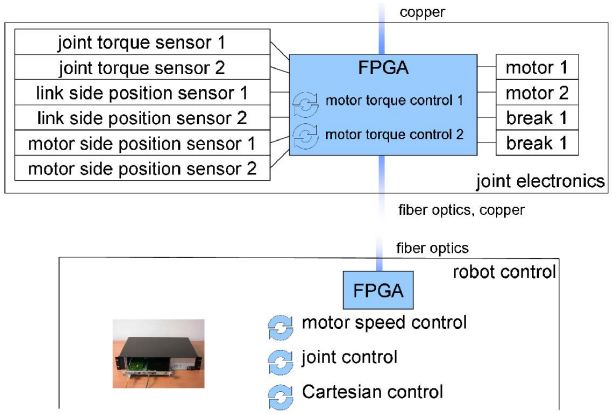

Fig. 8. Communication structure of the DLR medical robot: FPGAs as basic components for the communication and control of the joint units.

for the DLR light-weight robots the joint state control law software runs on the respective joint unit electronics of the robotic arm and calculations of the couplings between the joints are complex, for the medical robot new multi-joint controllers are used to operate the coupled joints. These state control laws allow a sensitive impedance control of the joints as well as stiff position control. The following sections briefly describe the chosen control strategy.

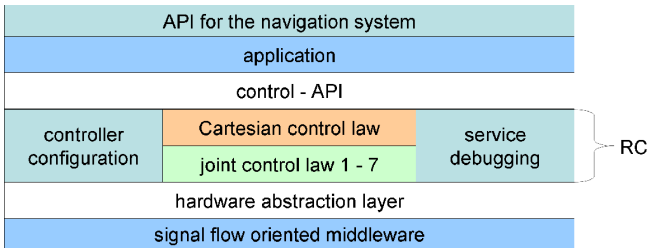

Fig. 9. Layer model of the robot control (RC): The complete robot control including the joint control is implemented on an external computer.

From a control point of view, the surgical robot shows a similarity to the DLR light-weight arms in many respects: high transmission reduction Harmonic-Drive gears, and joint torque sensors are applied as well as the joint elasticity is taken into consideration [12]. In the following a robot model is therefore considered in which the elasticity of the robot is treated in concentrated form as linear joint stiffness whilst the flexibility of the robot structure is disregarded [15]:

$$\begin{aligned} M(q)\ddot{q} + C(q,\dot{q})\dot{q} + g(q) &= \tau + \tau_{ext} \ , \\ B\ddot{\theta} + \tau &= \tau_m \ . \end{aligned}$$

In this equation $M(q)$ represents the inertia matrix, $C(q,\dot{q})\dot{q}$ the centrifugal and Coriolis terms and $g(q)$ the gravity torques of the link side rigid body model. In order to take account of the coupled joints the generalized motor

positions θ are introduced which are related to the physical motor angles θ_{phys} via a constant matrix T in the form $\theta = T\theta_{phys}$. The vector of the joint torques is given by $\tau = K(\theta - q)$, whereby q indicates the vector of the link side joint angles, and K the diagonal joint stiffness matrix. In addition, τ_{ext} are the external torques and τ_m the generalized motor torques which are regarded as input variables for the controller design. Dually to the relation $\theta = T\theta_{phys}$ the generalized motor torques τ_m are related to the physical motor torques τ_{phys} via $\tau_m = T^{-T}\tau_{phys}$. The matrix B is the diagonal[1] motor inertia matrix according to θ.

With regard to the presented application, Cartesian impedance control is particularly of interest. Here the goal is a defined impedance behaviour between external (generalized) forces acting on the robot and the end-effector movement. In the following it is assumed that the desired impedance can be specified by a stiffness matrix K_d and a damping matrix D_d. These matrices are defined with respect to a set of suitable Cartesian coordinates $x(q)$ which determine the pose of the end-effector. The corresponding Jacobian matrix is indicated with $J(q) = \partial x(q)/\partial q$. The desired virtual[2] equilibrium position is given by x_d.

For the robot arm basically the same control structures are used as they were designed for the DLR light-weight arms [16]–[19]. The Cartesian impedance controller from [17]–[19] is designed according to a cascaded control structure. An inner torque controller

$$\tau_m = \tau_d - K_t(\tau - \tau_d) - K_s\dot{\tau} \ , \qquad (1)$$

with positive definite matrices K_t and K_s obtains its desired torque τ_d from an outer impedance controller, Fig. 10.

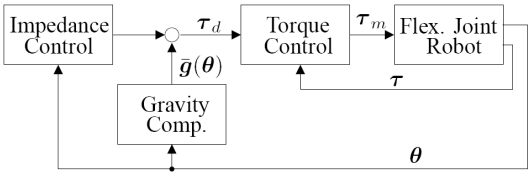

Fig. 10. Schematic diagram of the Cartesian impedance control consisting of an inner control loop for the joint torque τ and an outer control loop for the implementation of the desired Cartesian impedance behaviour.

The use of an inner torque controller has two advantages here. On the one hand a reduction of the effective inertia (from B to $(I + K_t)^{-1}B$) is caused by the feedback of the joint torque [17]–[19]. This has a positive effect on the damping of the outer impedance controller. On the other hand the influence of the motor side friction on the closed loop dynamics is also reduced by the inner torque controller since the joint torque sensors are placed link side.

[1]This matrix is diagonal, because the motor inertia values of each coupled joint are the same.

[2]In impedance control the setpoint usually is called a *virtual* equilibrium position since it should be reached only for the case of free motion.

In addition to the torque control law an outer controller is used in which the desired impedance behaviour is achieved. Similar to the classic impedance control law for rigid robots [20], this controller consists of a term for gravity compensation and a term for the desired stiffness and damping:

$$\tau_d = \bar{g}(\theta) - J(\theta)^T \left(K_d(x(\theta) - x_d) + D_d\dot{x}(\theta)\right) \ . \qquad (2)$$

Notice that for the calculation of the Cartesian position $x(\theta)$ the motor side positions θ are used, but not the link side positions q. In combination with the physical interpretation of the torque controller as a scaling of the motor inertia, this allows a stability analysis of the closed loop system based on the passivity properties of (2), see [17]–[19].

The first part of this control law corresponds to the gravity compensation term from [17], [18]. This term allows the compensation of the static effect of the link side acting gravity torques $g(q)$, based only on the measurement of the motor side positions. Here it must be noted that, in the case where no external forces are applied on the robot, the equilibrium condition $\tau = K(\theta - q) = g(q)$ must be fulfilled. This represents a static relation between the motor side and link side joint angles which can be solved iteratively for $q = \bar{q}(\theta)$. The term $\bar{g}(\theta)$ is then given by $\bar{g}(\theta) = g(\bar{q}(\theta))$.

Whereas the motor side damping in combination with the inner torque controller reduces the dynamic effects of the joint elasticities, the static effects still exist. Since the control law was formulated for the motor side positions, the desired stiffness K_d is also obtained by means of (2) only with respect to the motor side angles. At the link side this is primarily noticeable as a serial combination of the joint stiffness K with the Cartesian stiffness K_d. Locally the influence of the joint stiffness can be taken into account by an appropriate specification of the Cartesian stiffness K_d. As the stiffness of the robot is in many cases noticeably greater than the desired Cartesian stiffness, and the absolute Cartesian positioning accuracy in the presented application must be obtained not via the joint sensors but via a navigation system this approximation is very suitable here. In [21] an advanced controller structure was proposed which extends the above mentioned iterative calculation of the gravity compensation $\bar{g}(\theta)$ with the Cartesian stiffness so that the desired link side stiffness is reached exactly [21].

V. Conclusion and Outlook

The kinematically redundant robot presented in this paper enables a direct haptic interaction of the operator by using torque sensors in the joints. By means of impedance control it is possible to guide the robot along preoperatively planned trajectories to the target area (pose of the pedicle screws). Possible pose errors are captured by the intra-operative navigation system and corrected by the robot. Consequently, a precise intra-operative transfer of the operation planning into the operating theatre is possible - even by a less experienced

surgeon. The drilling itself is carried out manually by the surgeon whilst the robot controls the correct pose of the drill machine. In this way the surgeon has full control over the workflow and can flexibly react in the case of unexpected events. The robot itself is furthermore characterised by light-weight structure, sensor redundancy and large workspace so that it can be used for many other clinical applications.

In particular these include minimally invasive cardio- and abdominal surgery where the robotic arm is used as tele-manipulator. Here, at least two robot arms are equipped with minimally invasive instruments. In order to establish full manipulability in the patient, these instruments are equipped with two additional actuated DoF at the distal end, cf. Fig. 11, left. In addition, these instruments are equipped with a miniaturised force/torque sensor near the tip of the instrument [22], cf. Fig. 11, right. With this sensor the manipulation forces, which are hardly perceptible in manual minimally invasive surgery, can be measured.

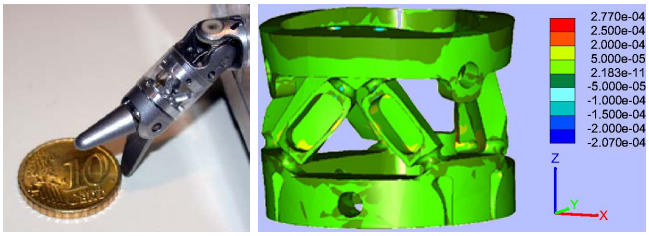

(a) Additional DoF (b) Miniaturised force/torque sensor

Fig. 11. Gripper for minimally invasive robotic surgery.

The measurement of manipulation forces allows a variety of new applications such as force controlled instrument holder, compensation of organ motion, supervision and limitation of forces applied to threads as well as feedback of the forces to the surgeon (haptic and/or visual), cf. [23].

ACKNOWLEDGMENTS

The authors would like to thank the Bavarian Research Foundation, the Bavarian Competence Network for Mechatronics, the German Research Foundation, and the company BrainLAB for their financial support. Special thanks also go to Prof. Beisse (BGU Murnau), Prof. Mittelmeier (Rostock University) as well as Dr. Burgkart, Dr. Steinhauser, and Dr. Schreiber (Technical University Munich, Clinic for Orthopaedics and Sport Orthopaedics) for support.

REFERENCES

[1] V. Falk. Robotic technology in cardiac surgery. *Applied Cardiopulmonary Pathophysology*, 10, 2001.

[2] S.D. Gertzbein and S.E. Robbins. Accuracy of pedicular screw placement in vivo. *Spine*, 16:181–184, 1990.

[3] L.H. Kuner, A. Kuner, W. Schlickewei, and B. Wimmer. Die Bedeutung der Ligamentotaxis für die Fixateur interne Osteosynthese bei Frakturen der Brust- und Lendenwirbelsäule. *Chirurg*, 63:50–55, 1992.

[4] E. Sim. Location of transpedicular screws for fixation of the lower thoracic and lumbar spine. Computed tomography of 45 fracture cases. *Acta Orthop Scand*, 64:28–32, 1993.

[5] A.R. Vaccaro, S.J. Rizzolo, R.A. Balderston, T.J.. Allardyce, S.R. Garfin, and C. Dolinskas. Placement of pedicle screws in the thoracic spine. Part II: an anatomical and radiographic assessment. *Bone Joint Surg*, 77:1200–1206, 1995.

[6] Russell H. Taylor and Dan Stoianovici. Medical robotics in compter-integrated surgery. *IEEE Transactions on Robotics and Automation*, 19(5):765–781, 2003.

[7] G. Guthart and J. Salisbury. The Intuitive telesurgery system: Overview and application. In *IEEE International Conference on Robotics and Automation (ICRA)*, pages 618–621, San Francisco, USA, April 2000.

[8] Jonathan M. Sackier and Yulun Wang. *Computer-Integrated Surgery*, chapter Robotically Assisted Laparoscopic Surgery: From Concept to Development, pages 577–580. MIT Press, 1995.

[9] J.-S. Hong, T. Dohi, M. Hashizume, K. Konishi, and N. Hata. A motion adaptable needle placement instrument based on tumor specific ultrasonic image segmentation. In *Medical Image Computing and Computer-Assisted Intervention - MICCAI 2002: 5th International Conference, Proceedings*, Tokyo, Japan, September 2002.

[10] M. Jakopec, S.J. Harris, F.R. y Baena, P. Gomes, J. Cobb, and B.L. Davies. Preliminary results of an early clinical experience with the Acrobot system for total knee replacement surgery. In *Medical Image Computing and Computer-Assisted Intervention - MICCAI 2002: 5th International Conference, Proceedings*, Tokyo, Japan, September 2002.

[11] G.-Q. Wei, K. Arbter, and G. Hirzinger. Real-time visual servoing for laparoscopic surgery. *IEEE Engineering in Medicine and Biology*, 16(1):40–45, January/February 1997.

[12] G. Hirzinger, A. Albu-Schäffer, M. Hähnle, I. Schaefer, and N. Sporer. On a new generation of torque controlled light-weight robots. In *IEEE International Conference of Robotics and Automation*, pages 3356–3363, 2001.

[13] R. Konietschke, T. Ortmaier, H. Weiss, R. Engelke, and G. Hirzinger. Optimal design of a medical robot for minimally invasive surgery. In *Proceedings of the 2nd Conference of the German Society of Computer and Robotic Assisted Surgery (CURAC)*, Nürnberg, Germany, November 2003.

[14] P. Lemke and G. Hirzinger. Auslegungsoptimierung einer hochpoligen einzelpolbewickelten permanenterregten Synchronmaschine. In *Elektrisch-mechanische Antriebssysteme, Innovationen - Trends - Mechatronik*, Fulda, October 2004. VDI/VDE.

[15] M.W. Spong. Modeling and control of elastic joint robots. *Transactions of the ASME: Journal of Dynamic Systems, Measurement, and Control*, 109:310–319, 1987.

[16] A. Albu-Schäffer. *Regelung von Robotern mit elastischen Gelenken am Beispiel der DLR-Leichtbauarme*. PhD thesis, Technische Universität München, 2001.

[17] Ch. Ott, A. Albu-Schäffer, A. Kugi, S. Stramigioli, and G. Hirzinger. Kartesische Impedanzregelung von Robotern mit elastischen Gelenken: Ein passivitätsbasierter Ansatz. *at-Automatisierungstechnik*, pages 378–388, 8 2005.

[18] Ch. Ott, A. Albu-Schäffer, A. Kugi, S. Stramigioli, and G. Hirzinger. A passivity based Cartesian impedance controller - part I: Torque feedback and gravity compensation. In *Proceedings of the 2004 IEEE International Conference on Robotics and Automation*, pages 2659–2665, 2004.

[19] A. Albu-Schäffer, Ch. Ott, and G. Hirzinger. A passivity based Cartesian impedance controller - part II: Full state feedback, impedance design and experiments. In *Proceedings of the 2004 IEEE International Conference on Robotics and Automation*, pages 2666–2672, 2004.

[20] N. Hogan. Impedance control: An approach to manipulation, part I-III. *ASME Journal of Dynamic Systems, Measurement, and Control*, 107:1–24, 1985.

[21] A. Albu-Schäffer, Ch. Ott, and G. Hirzinger. Passivity based cartesian impedance control for flexible joint manipulators. In *IFAC Symposium on Nonlinear Control Systems (NOLCOS)*, 2004.

[22] U. Seibold, B. Kübler, and G. Hirzinger. Prototype of instrument for minimally invasive surgery with 6-axis force sensing capability. In *IEEE International Conference on Robotics and Automation (ICRA)*, Barcelona, Spain, April 2005.

[23] T. Ortmaier. *Motion Compensation in Minimally Invasive Robotic Surgery*. VDI Verlag, 2003. PhD Thesis.